A R C H I V E S O F M E T A L L U R G Y A N D M A T E R I A L S
Volume 50 2005 Issue 2

Z. JASIEŃSKI*, H. PAUL*, J. DRIVER**, A. PIĄTKOWSKI*, A. LITWORA*

INFLUENCE OF THE CHANGE OF THE DEFORMATION PATH ON DEFORMATION BANDING IN Cu-8%Al ALLOY SINGLE CRYSTALS

WPŁYW ZMIANY DROGI ODKSZTAŁCENIA NA PASMOWĄ LOKALIZACJĘ ODKSZTAŁCENIA W MONOKRYSZTAŁACH STOPU Cu-Al8%WT

The textural and microstructural effects of cross rolling of fcc metals with low stacking fault energy have been studied by local orientation measurements in the SEM equipped with field emission gun (FEG) and by X-ray pole figure measurements. The analysis is focused on shear bands and deformation bands development by plane strain compression in copper-8%wt. aluminium alloy single crystals with twinned C{112}<111> and non twinned CR{112}<110> orientations as well as in twinned CRP{112}<110> samples after changing of the deformation path as a result of 90°ND||< 112 > rotation. It has been found that important transitions of the deformation textures are correlated with deformation banding. In C{112}<111>-oriented samples and in those after the change of the deformation path (i.e. in {112}<110> pre-deformed as {112}<111>) the high resolution SEMFEG orientation maps allowed investigation of the way in which unstable behaviour of twin-matrix layers leads to the"brass"-type shear bands and formation of the deformation bands. Within well-developed shear bands the dominance of crystal lattice rotation about one of the <112> poles was observed. This is correlated with the operation of one of the two, initially equally active co-planar slip systems of {111}<110>-type. As a consequence, the rotation of twinned areas within shear bands is observed. This ultimately leads to formation of texture components near the B{110}< 112 >-S{123}<634 > fibre. In non- twinned CR{112}< 110 > orientation from the beginning stages of deformation, a strong tendency to decomposition as a result of <112> rotation is also clearly observed. This leads to another type of deformation bands resembling the transition ones. From crystallographic point of view the tendency to form two nearly complementary positions of B{110}<112> orientation is observed.

Teksturowe i mikrostrukturalne efekty walcowania krzyżowego metali o sieci A1 i niskiej energii błędu ułożenia badano metodą pomiaru pojedynczych orientacji w mikroskopie skaningowym (SEM) wyposażonym w działo polowe (FEG) jak również metodą

* INSTYTUT METALURGII I INŻYNIERII MATERIAŁOWEJ IM. A, KRUPKOWSKIEGO, POLSKA AKADEMIA NAUK, 30-059 KRAKÓW, UL. REYMONTA 25

** ECOLE NATIONALE SUPERIEURE DES MINES DE ST.ETIENNE, 158 COURS FAURIEL, 42023 SAINT ETIENNE CEDEX 2, FRANCE

dyfrakcji rentgenowskiej. Analizowano rozwój pasm ścinania i pasm odkształcenia podczas nieswobodnego ściskania monokryształów stopu Cu-Al8% wag., posiadających początkową orientację C{112}<111> sprzyjającą bliźniakowaniu odkształceniowemu i orientację CR{112}<110> nie bliźniakującą, jak również w zbliźniaczonych próbkach orientacji CRP{112}<110> t.j. wstępnie odkształconych w położeniu C i obróconych 90° wokół ND||<112> (ściskanych po zmianie drogi odkształcenia). Stwierdzono, że silne transformacje tekstury odkształconych próbek związane są z pasmową lokalizacją odkształcenia. W próbkach o początkowej orientacji C oraz w próbkach CRP odkształconych po zmianie drogi deformacji (wstępna deformacja w położeniu C), otrzymane mapy orientacji metodą SEM/FEG umożliwiły pełną charakterystykę krystalograficznych cech rozwoju pasm ścinania typu mosiądzu oraz tworzenia pasm odkształcenia. W pasmach ścinania wykazano dominację obrotów sieci wokół osi <112>leżących w płaszczyźnie dwóch równoważnie aktywnych systemów współpłaszczyznowych BII i BIV, co prowadzi do rozwoju własnej lokalnej tekstury pasma ścinania charakteryzującej się składowymi tekstury walcowania mosiądzu G{110}<001>, B{110}<112> z udziałem składowej S{123}<634>. W przypadku nie zbliźniaczonej orientacji CR{112}<110> obrót wokół osi <112> leżących w płaszczyznach dwóch niekoplanarnych, równoważnie aktywnych systemów AIII i DI prowadzi również do powstania dwóch komplementarnych składowych B{110}<112> charakteryzujących alternatywnie orientację sąsiednich pasm odkształcenia, powstających w wyniku alternatywnego operowania pojedynczych systemów poślizgu.

1. Introduction

The present work aims to characterize the role of deformation banding in the texture evolution of cross-rolled fcc metals with low SFE and to assess the influence of initial orientation on the crystallographic nature of the occurring inhomogeneities in the form of shear bands (SBs) and/or deformation bands (DB). The textural effect of the change of the deformation path by 90° rotation about normal direction (ND) in copper – 8% wt. aluminium alloy single crystals was investigated by a channel- die compression test, modelling the plane state of strain and on this account representing an approach to the rolling process. The microstructures and the local orientation changes in twinned C(112)[11$\bar{1}$] and non twinned CR(112)[1$\bar{1}$0] orientation as well as in twinned CRP(112)[1$\bar{1}$0] samples after changing of the deformation path (where ND2=ND1//-<112>, ED2=TD1 and TD2=ED1) have been characterized on the longitudinal sections by local orientation measurement in the SEM equipped with field emission gun (FEG) as well as X-ray diffraction for the global texture determination.

According to the previous studies [1, 2], in the C-orientation a specific configuration of two co-planar and two co-directional privileged slip systems favours the development of typical shear bands. Instead, the symmetrical configuration of two conjugated single slip systems in CR-orientation is disadvantageous for the development of SBs. Accepting the assumption of homogeneous slip in f.c.c. metals, the numerical simulation [5] has shown that the orientation {112}<110> is instable and during cold-rolling it rotates towards the B{110}<112> position.

2. Experimental procedures

The investigations were carried out on copper — 8% wt. aluminium alloy single crystals obtained by a modified Bridgman method at the Department of Structure and Mechanics of Solid Body of AGH — University of Science and Technology. Cubic samples have been used with the edge length of 10mm, cut with a wire saw from the supplied prisms 10.2mm by 10.2mm by 100mm in size. The sample walls were chemically and electrolytically polished and then covered with a Teflon foil to reduce the effects of friction in the channel-die test.

The samples were channel-die compressed with an INSTRON 6025 tensile testing machine. The value of the load and the change of the sample thickness (distance covered by the traverse of the testing machine) were recorded. In the case of a change of the deformation path, the front and the back parts of the samples were cut off perpendicular to elongation direction (ED); the distance between the parts was 10mm. The performed investigations comprised two kinds of the single crystals experiments on samples of the following orientations (Fig 1):

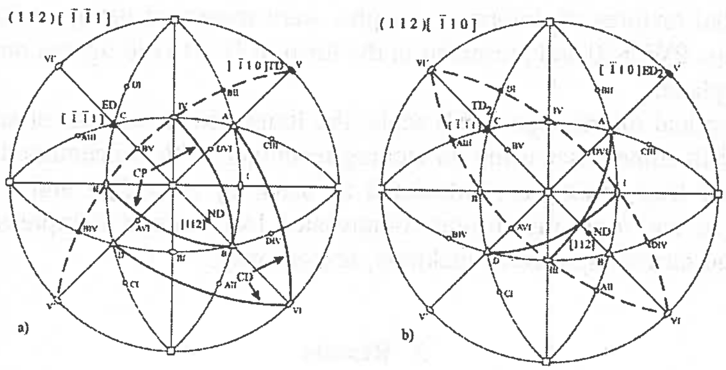

Fig. 1. Stereographic (001) projection showing the active slip systems in channel-die compressed single crystals. (a) C(112)[$\bar{1}\bar{1}$1] orientation — the co-planar systems: BII, BIV, and co-linear systems: AVI, DVI. (b) CR(112)[$\bar{1}$10] orientation — single slip systems: AIII and DI

— C(112)[11$\bar{1}$] (the so-called "copper" or C orientation) and CR(112)[1$\bar{1}$0] — initially oriented samples were subjected to channel-die compression without changing of the deformation path to a reductions of 47% and 22.5%, respectively. The applied reductions determine the formation of well-defined clusters of MSB at 21.2% of reduction (for C orientation) and deformation bands (in the case of CR orientation). It is clearly visible that there exists a strictly defined, simple relation between both sample orientations connected with 90°ND||<112> rotation.

— C(112)[11$\bar{1}$]-oriented sample was pre-deformed in at first stage up to 20.7%, until a broad band of deformation twins was formed. Then the sample was rotated 90° about ND||<112> direction (CRP (112)[1$\bar{1}$0]-orientation) and additionally compressed to 32.1% reduction. In the case of CRP (112)[1$\bar{1}$0] oriented sample, the interrelations between external axes were as follows: ND1=ND2||<112>, ED2=TD1||<110> and TD2=ED1||<111>. The applied deformations were such that within the different areas of the samples one or two sets of coarse slip bands were observed.

The deformation microstructures and microtextures were characterized by EBSD/SEM-FEG in a JOEL JSM 6500F scanning electron microscope equipped with a field emission gun. Microscope control, pattern acquisition and solution were carried out with the HKL Channel 5 system. To reveal the crystallographic contrast the backscattered electrons at 15kV were used. The diffraction data were acquired as orientation maps usually using raster scans 400×300 pixels, with different size of 0.2-0.5μm, and the acquisition time ~0.02-0.05 s/pattern.

The SEM samples were sectioned in planes perpendicular to TD (or TD2 after changing of the deformation path). Local orientation data obtained by SEMFEG/EBSD technique on the ND- ED plane were transformed to the standard ED-TD reference system and presented in the form of {111} pole figures.

The global textures of deformed samples were measured using an X-ray diffractometer Philips PW1830 and presented in the form of {111} pole figures on the ND-ED longitudinal plane.

On the optical microscope (OM) scale, the longitudinal sections of samples were characterized in some cases using an etching technique with concentrated nitric acid.

Stress and true strain were calculated as usual by $\sigma = F/A$ and $\varepsilon = ln(h_o/h)$, where F, A, h_o and h are the current compression load, sample compression surface, and initial and current specimen thickness, respectively.

3. Results

Stress strain behaviour. The experimental true stress-strain curves for C(112)[11$\bar{1}$] and CRP (112)[1$\bar{1}$0] oriented crystals (Fig.2a and c) after an initial deformation of about 0.20-0.25 exhibit the stress serration's, typical of deformation twinning.

The concentration of twins in a broad band, initially inclined at about 25°- 27° to ED and clearly observed in the longitudinal plane (Fig.3a), indicates that twinning starts on (111) coplanar slip plane from orientations which have deviated from the initial C-orientation towards the so-called Dillamore component D(4 4 11)[11 11 $\bar{8}$]. This is confirmed by X-ray {111} pole figure of Fig.3c, which shows the twin orientation DT(26 26 5)[$\bar{5}$ $\bar{5}$ 52]. At higher strains the large wavy stress drops are associated with the development of macroscopically visible clusters of SBs (at the sample scale — Fig. 3a). The exhaustion of deformation by deformation twinning induces the rotation of the twinning planes towards the compression plane. It coincides with the initial stage of strain localization in the so-called brass-type shear bands. They occur inside of the characteristic broad kinks of twinning planes usually inclined at an angle of about 40°-45° to ED and parallel to the TD axis [3].

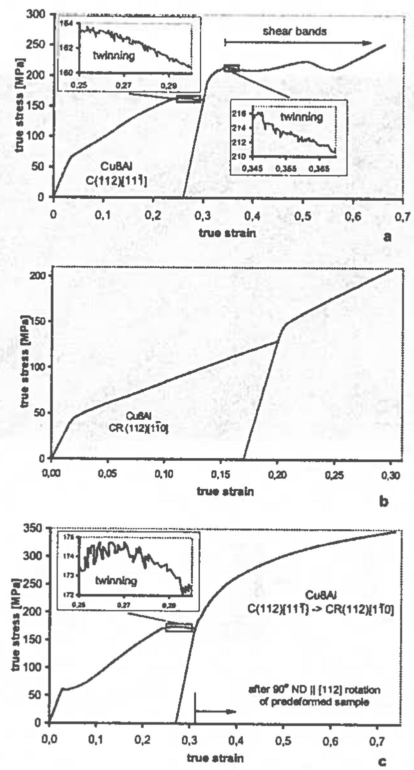

Fig. 2. True stress-strain curves for channel-die deformed single crystals of Cu-8%Al alloy. (a) C(112)[11$\bar{1}$] orientation, (b) CR(112)[1$\bar{1}$0] orientation, (c) CRP(112)[1$\bar{1}$0] orientation (pre-deformed to 20.7% reduction in C(112)[11$\bar{1}$])

The true stress-strain curves for CR(112)[1$\bar{1}$0] initially oriented crystals (Fig. 2b) and for pre-deformed CRP-oriented crystals after changing of the deformation path by 90°ND||[112] rotation (Fig.2c) show a monotonic increase of stress as a function of strain. The stress-strain behaviour of initially CR-oriented single crystals (Fig. 2b) indicate that the deformation twinning and shear banding have never occurred. However, these orientations show a strong tendency to fragmentation and/or formation of the band like — inhomogeneities as observed macroscopically in Fig.4a and 5a. The X-ray {111} pole figures show a clearly defined tendency to decomposition of the initial CR-orientation and pre-deformed CRP-orientation towards the B{110}<112> position (Fig. 4b and 5b).

Local orientations. In the C(112)[11$\bar{1}$] oriented single crystals, the macroscopically observed brass-type shear bands (MSBs) are composed of a single set of highly localized bands, as shown by the orientation imaging map (OIM) in Fig. 6a. These MSBs are rather irregularly spaced and their positions correspond to the darker longitudinal areas (lower image quality factor) in ND-ED plane. The orientation scans within the MSBs area (Fig. 6b) reveal large orientation spreads of up to 35° in the SBs. Most of

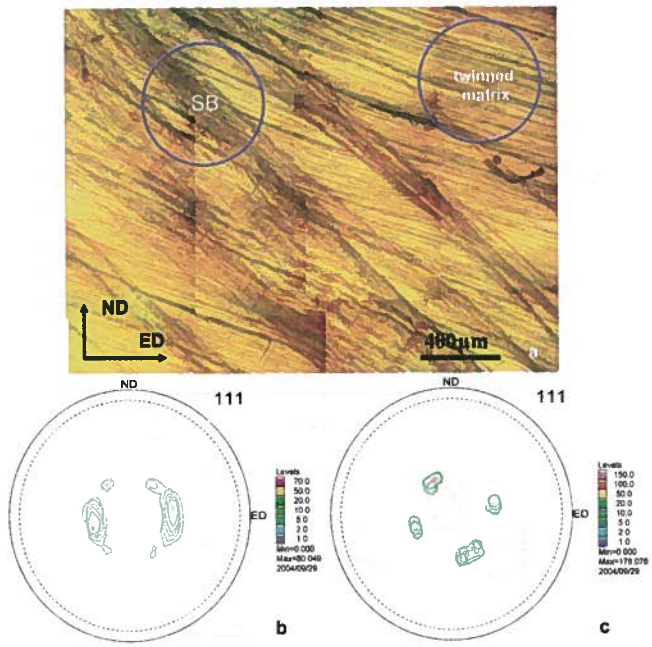

Fig. 3. Cu-8%Al alloy single crystal of twinned C(112)[11$\bar{1}$] orientation deformed 47%. (a) Macroscopic shear bands within twinned matrix structure observed by optical metallography in the longitudinal (ND-ED) plane. SB-shear band. (b) and (c) {111} pole figures determined by X-ray diffraction in shear band area and in twinned matrix area respectively. Longitudinal (ND-ED) reference plane

these misorientations occur about the TD<110> axis but, as observed on the {111} pole figure of entire OIM (Fig. 6a), there are significant further rotations about one of the two <112> axes close to TD axis. Thus the slip on the two coplanar systems in the SBs becomes asymmetric, i.e. the rotation about one of the two <112> axes corresponds to preferred single slip on one of the two coplanar BII or BIV slip systems. These effects are clearly visible on the essential part of the misorientation axes distribution presented in Fig. 3e, where the scattering of the axes between the <110> and <112> directions is observed. The {111} pole figure and the inverse pole figures of the ND and ED axes (Fig. 6c) clearly demonstrate the dominance of the Goss-{110}<001> microtexture component of a single MSB (Fig. 6d). Moreover, in some areas the near primary matrix orientation {114}<221> was occasionally observed. The presence of the near-Goss position indicates that within SBs areas the normal of the (111) plane are more inclined to ND than in the adjacent areas outside the SBs. This is evidence that the progressive rotation within the SBs brings the (111) twinning planes into a position parallel to the shear plane.

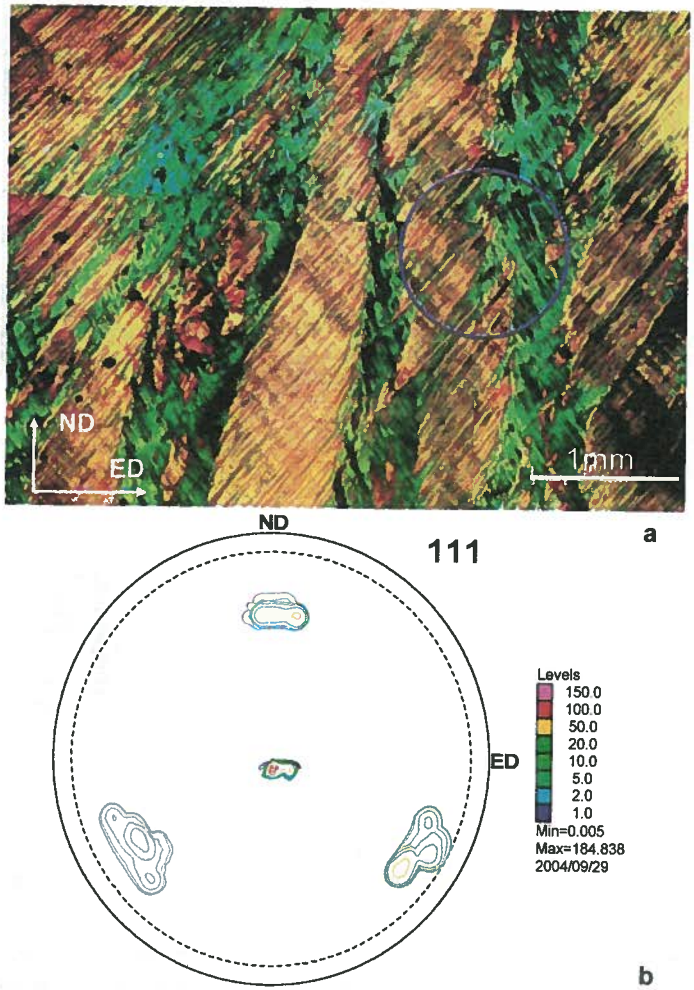

Fig. 4. Cu-8%Al alloy single crystal of non-twinned CR(112)[1$\bar{1}$0] initial orientation after 22.5% reduction. (a) Banded microstructure observed in the longitudinal (ND- ED) plane. (c) {111} pole figure determined by X-ray diffraction in longitudinal (ND- ED) reference plane

The CR(112)[1$\bar{1}$0] oriented single crystals are very unstable as a whole and show a strong tendency to fragmentation in the form of macroscopically observed band-like strain inhomogeneities (Fig.4a). In the orientation imaging map (Fig. 7a) two differently inclined families of elongated areas are observed in which only one of the two privileged slip systems AIII or DI is predominantly operating. As a consequence, the progressive change of the initial orientation inside this selected area occurs by rotation about the <112> axis close to the TD. This interpretation is supported by the essential part of the misorientation axes distribution with misorientation angles of 20°-25° (Fig. 7d). The {111} pole figure in Fig. 7c shows a distinct tendency of scattering of the

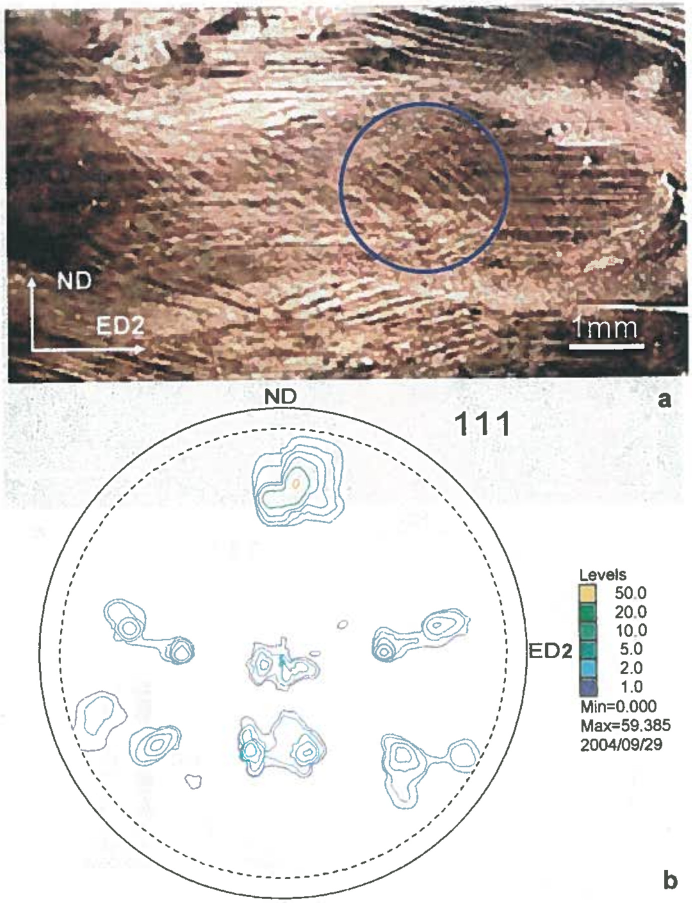

Fig. 5. Cu-8%Al alloy single crystal of CRP(112)[1 0] twinned orientation (pre-deformed in C-orientation). (a) Global view of longitudinal (ND-ED) plane of deformed 32.1% CRP-sample after 90°ND||[112] rotation. (b) {111} pole figure determined by X-ray diffraction in (ND-ED) reference plane, showing the twin component of global texture

poles towards the B{110}<112> position. This tendency is more clearly shown on inverse pole figures (Fig. 7b), where the strong scattering of ND towards the <110> and ED towards the <112> are observed.

In the case of the twinned CRP(112)[1$\bar{1}$0] samples (pre-deformed in (112)[11$\bar{1}$] position) the fragmentation of the microstructure is observed in the form of irregular deformation bands crossing the single family of straight twin lamellae (Fig. 8a). These specific deformation bands of complementary orientations are separated by the wavy, high angle boundaries. The misorientation created across the boundary is usually 20°- 30° (Fig. 8d). The {111} pole figure of entire OIM shows a distinct tendency of scattering towards the complementary B{110}<112> positions (Fig. 8c). The tendency

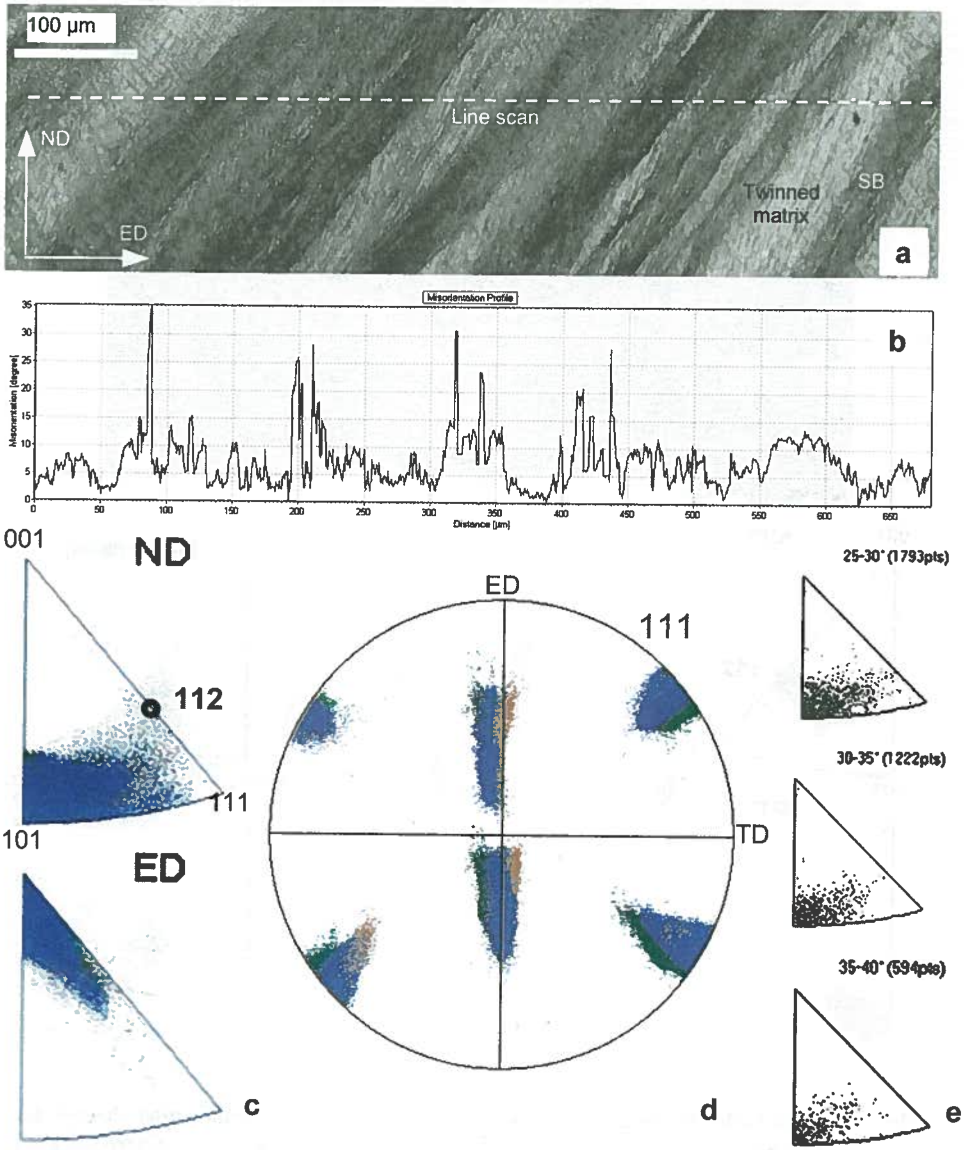

Fig. 6. Cu-8%Al alloy single crystal of the initial C(112)[11] orientation after channel-die compression of 47%. (a) Orientation imaging map. Darker areas characterise the SB positions. (b) Misorientation profile with respect to the first measured point along an ED line scan presented in (a) at $1\mu m$ intervals. (c) Inverse pole figures of the ND and ED axes. (d) {111} pole figure from (a). (e) Essential part of the distribution of the misorientation axes

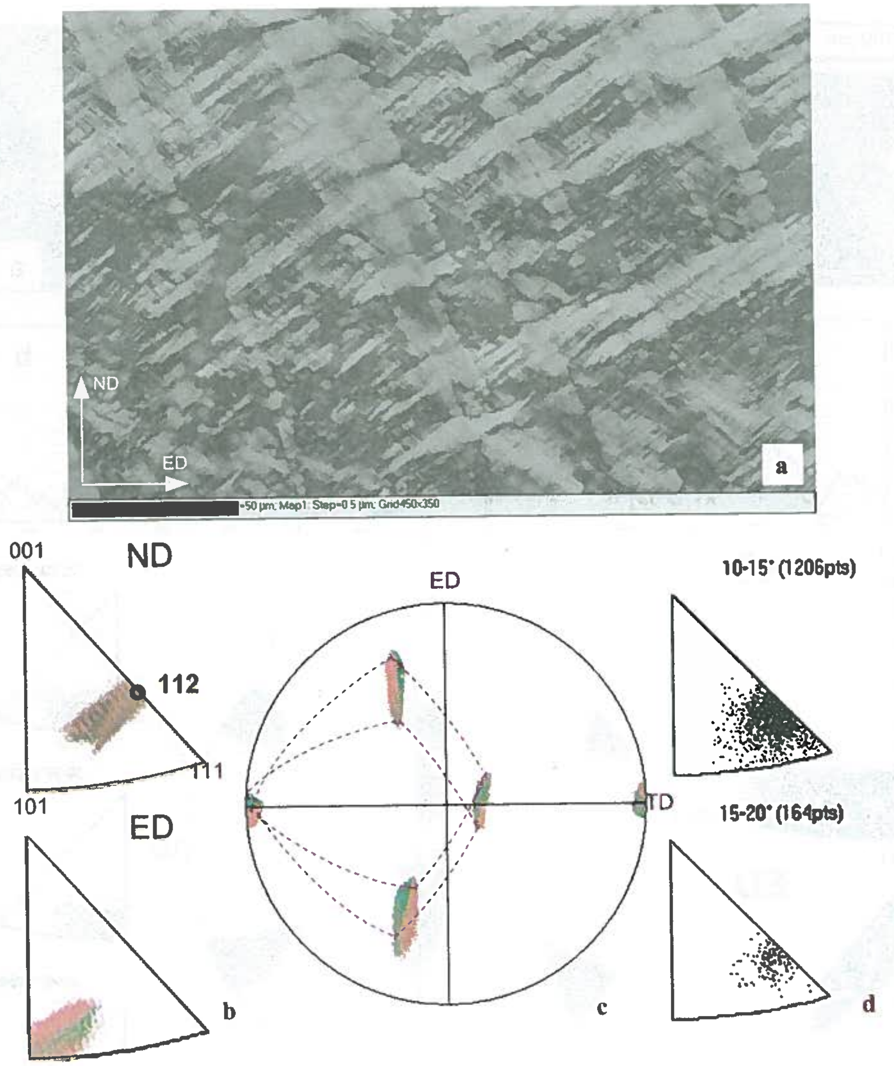

Fig. 7. Cu-8%Al alloy single crystal of the initial CR(112)[$1\bar{1}0$] orientation after channel-die compression of 22.5%. (a) Orientation imaging map. (b) Inverse pole figures of the ND and ED axes. (c) {111} pole figure from (a). (d) Essential part of the distribution of the misorientation axes

is more clearly shown on inverse pole figures (Fig. 8b), where the strong scatterings of ND towards the <110> and ED2 towards the <112> are observed. The progressive alternating changes of orientation inside the particular deformation bands are induced by selected activity of only one of the two privileged non-coplanar slip systems AIII or DI. As a consequence, the axes of 20°-30° rotations in each band are the directions [$\bar{2}\bar{1}1$] or [$\bar{1}\bar{2}1$] respectively, situated near the TD2||[$\bar{1}\bar{1}1$] direction. Such a behaviour differs from that of macroscopic shear bands, as characterized in the previous investigations [1, 2, 4].

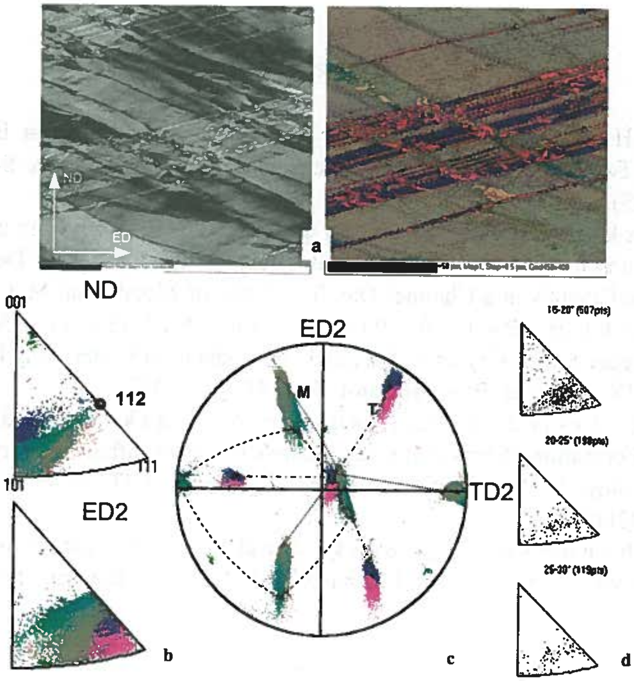

Fig. 8. Cu-8%Al alloy single crystal of the CRP(112)[1$\bar{1}$0] (pre- deformed in C-orientation and rotated by 90° ND) after an additional reduction to 32.1%. (a) The so-called Schmid factor map (left) and orientation imaging map (right). (b) Inverse pole figures of the ND and ED axes from OIM in (a-right). (c) {111} pole figure from (a-right).(d) Essential part of the distribution of the misorientation axes

4. Conclusions

1. The destabilization of the CR(112)[1$\bar{1}$0] orientation during channel-die compression leads to the B{110}<112> preferred orientation. It has been shown that this type of texture transformation occurs in pre-deformed (twinned) CRP-oriented samples as well as in those with the non-twinned CR-orientation.

2. The localization of deformation in the form of typical brass-type shear bands depends on the initial orientation of a single crystal. The coplanar configuration of two preferred slip systems plays a decisive role in the formation of the typical SBs. The non-coplanar configuration of two single slip systems prohibits the development of SBs.

Acknowledgements

This work was partly supported financially by the Polish Committee for Scientific Research (KBN), project No 7 T08A 062 21

REFERENCES

[1] H. Paul, J.H. Driver, C. Maurice, Z. Jasieński, Shear Band Microtexture Formation in Twinned Face Centered Cubic Single Crystals, Materials. Sci. and Eng. **A359** 178-191 (2003).

[2] Z. Jasieński, J. Pospiech, A. Piątkowski, R. Schwarzer, A. Litwora, M. Ostafin, Textural and Structural Effects of the Change of Deformation Path in Copper Single Crystals in a Channel-Die Test, Arch. of Metall. and Mat. **49**, 11-28 (2004).

[3] Z. Jasieński, H. Paul, A. Piątkowski, A. Litwora, Microstructure and Texture of Copper Single Crystals of (112)[111] Orientation Undergoing Channel-Die Compression at 77K, J. Mater. Proc. Technol. **53**, 187-194 (1995).

[4] H. Paul, Z. Jasieński, C. Maurice, A. Piątkowski, J.H. Driver, A. Litwora, Formation of brass-type shear bands and their influence on orientation changes of Cu-2%Al alloy {112}<111> single crystals, Rev.Metal.–CIT/Sci. et Génie des Matériaux **11**, 797-805 (2003).

[5] K. Wierzbanowski, Jasieński, Simulation numérique de la déformation d'un cristallite individuel au cours de laminage, Bull. Acad. Polon.Sci., Ser.sci.techn. **25**, 67 [543] (1977).

Received: 21 March 2005.